

The H2M Monolithic Active Pixel Sensor — characterizing non-uniform in-pixel response in a 65 nm CMOS imaging technology

S. Ruiz Daza,^{a,1} R. Ballabriga,^b E. Buschmann,^c M. Campbell,^b R. Casanova Mohr,^d
D. Dannheim,^b J. Dilg,^a A. Dorda,^b F. King,^a O. Feyens,^a P. Gadow,^b I.M. Gregor,^a
K. Hansen,^a Y. He,^a L. Huth,^a I. Kremastiotis,^b C. Lemoine,^{b,2} S. Maffessanti,^a
L. Mendes,^a Y. Otari,^b C. Reckleben,^a S. Rettie,^b M.A. del Rio Viera,^a J. Schlaadt,^a
A. Simancas,^a W. Snoeys,^b S. Spannagel,^a T. Vanat,^a A. Velyka,^a G. Vignola,^a
H. Wennl f^{a,3}

^a*Deutsches Elektronen-Synchrotron DESY,
Notkestr. 85, 22607 Hamburg, Germany*

^b*CERN,
Esplanade des Particules 1, Geneva, Switzerland*

^c*Brookhaven National Laboratory (BNL),
New York 11973-5000, Upton, USA*

^d*Institut de F sica d'Altes Energies (IFAE),
Edifici CN, UAB campus, 08193 Bellaterra (Barcelona), Spain*

E-mail: sara.ruiz.daza@desy.de

ABSTRACT: The high energy physics community recently gained access to the TPSCo 65 nm ISC (Image Sensor CMOS), which enables a higher in-pixel logic density in monolithic active pixel sensors (MAPS) compared to processes with larger feature sizes. To explore this novel technology, the Hybrid-to-Monolithic (H2M) test chip has been designed and manufactured. The design followed a digital-on-top design workflow and ports a hybrid pixel-detector architecture, with digital pulse processing in each pixel, into a monolithic chip. The chip matrix consists of 64×16 square pixels with a size of 35×35 μm², and a total active area of approximately 1.25 mm². The chip has been successfully integrated into the Caribou DAQ system. It is fully functional, and the measured threshold dispersion and noise agree with the expectation from front-end simulations. However, a non-uniform in-pixel response related to the size and location of the n-wells in the analog circuitry has been observed in test beam measurements and will be discussed in this contribution. This asymmetry in the pixel response, enhanced by the 35 μm pixel pitch — larger than in other prototypes — and certain features of the readout circuit, has not been observed in prototypes with smaller pixel pitches in this technology.

KEYWORDS: Particle tracking detectors (Solid-state detectors), Pixelated detectors and associated VLSI electronics

¹Corresponding author.

²Also at Universit  de Strasbourg, France.

³Now at Nikhef, Amsterdam.

1 Introduction

Monolithic CMOS sensors enable the development of detectors with a low material budget and a low fabrication cost. By using a small collection electrode, these sensors achieve small capacitance, low analog power consumption, and an improved signal-to-noise ratio. The availability of a 65 nm CMOS imaging process to the high-energy physics community further enhances their potential by allowing a higher density of in-pixel logic in monolithic active pixel sensors (MAPS) compared to processes with larger feature sizes. This 65 nm process has been previously explored in prototypes such as the APTS [1] and DPTS [2].

The H2M (Hybrid-to-Monolithic) test chip has been developed to demonstrate the capabilities of the 65 nm CMOS imaging process in tracking applications for future high-energy lepton experiments, while also addressing the challenges of porting a hybrid architecture into a monolithic chip, and testing a compact digital cell library and a complex and fast in-pixel readout circuitry.

2 The H2M test chip

The H2M sensor is manufactured using a modified TPSCo 65 nm ISC (Image Sensor CMOS). It comprises a small n-type collection electrode placed on a high-resistivity p-type epitaxial layer, which is grown on a low-resistivity substrate. To enhance charge collection in the sensitive layer with a thickness of $\sim 10 \mu\text{m}$, process modifications have been implemented, including a low-dose n-type implant with a gap at the pixel boundaries [3]. The wafers are backside-thinned to $50 \mu\text{m}$ physical thickness. A schematic of the sensor layout is illustrated in figure 1.

The chip matrix consists of 64×16 square pixels with a size of $35 \times 35 \mu\text{m}^2$, resulting in a total active area of approximately 1.25 mm^2 . Each pixel includes an analog front end that comprises a charge-sensitive amplifier (CSA) with Krummenacher feedback [4] followed by a discriminator. The design ensures a constant slope of the falling edge of the CSA output, adjustable through the Krummenacher feedback current (i_{krum}). The global threshold of the discriminator is selected with an 8-bit DAC, and threshold mismatch is compensated using a 4-bit threshold-tuning DAC per pixel. Individual pixels can be masked, and if needed, test pulses of varying amplitudes can

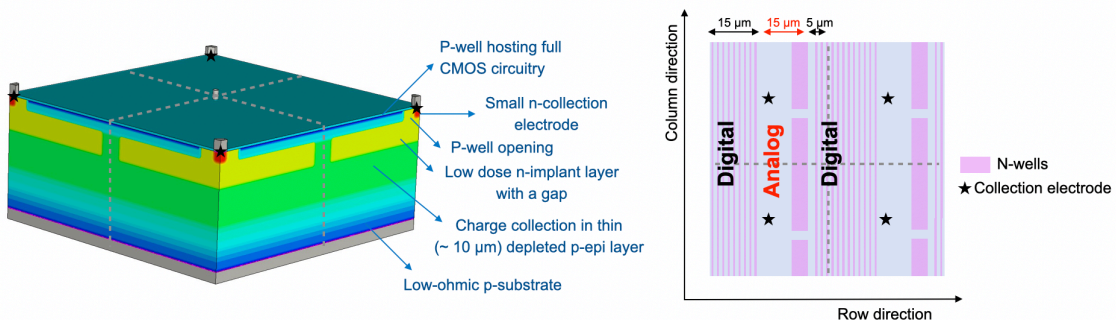


Figure 1: Schematic of the sensor layout on the left. The position of the digital and analog circuitry, as well as the position of n-wells therein, are schematically shown from a top view on the right. The pixel cell boundary is marked with a dashed gray line.

be injected before the CSA. The digital logic processes the output of the discriminator. Both the CMOS analog and digital front ends are hosted within the deep p-wells. The analog front-end begins at the collection electrode and extends 15 μm in the row direction, with the remaining space occupied by the digital readout circuitry. PMOS devices are shielded in n-wells inside the deep p-well.

The chip can operate in four non-simultaneous acquisition modes: 8-bit Time-over-Threshold (ToT) for energy measurements, 8-bit Time-of-Arrival (ToA) with 10 ns binning for time measurements, photon counting, and triggered mode. ToA represents the time of the threshold crossings as the charge is collected, while the ToT is the duration of the signal above the threshold. Photon counting mode counts hits above the threshold. In triggered mode, a binary readout occurs after hit validation by an external trigger signal, using an 8-bit delay counter to accommodate the trigger delay. The readout is integrated into the Caribou DAQ system [5]. It uses a 40 MHz clock and is frame-based without zero suppression.

The chip is fully functional, and it has been calibrated using radioactive sources. A single-pixel noise of 33 electrons r.m.s. and a threshold dispersion of the equalized matrix of 45 electrons have been measured, which agrees with the expectations from the front-end simulations.

3 Performance in test beam

To study the performance of H2M in terms of particle detection, the chip has been tested at the DESY II test beam facility [6], using the ADENIUM telescope [7] for particle tracking, and the Telepix2 detector serving as reference trigger and timing detector [8]. For data analysis, the Corryvreckan framework is used [9].

Figure 2a shows the efficiency and fake hit rate as a function of the hit detection threshold for three different bias voltages. The bias voltage on the p-well/substrate influences the depletion of the sensor volume. At low bias voltages ($< 2\text{ V}$), the area surrounding the collection electrode is not fully depleted, which increases the sensor capacitance and, consequently, noise and fake hit rate. Allpix² simulations, using the results from Technology computer-aided design (TCAD) simulations based on generic profiles [10], are performed to obtain the efficiency as a function of the detection threshold, which is also included in figure 2a. The difference between the measured and simulated efficiency can be explained by a non-uniformity in the in-pixel response, which will be further discussed below.

Figure 3a and 3b show the efficiency and ToA as a function of the in-pixel hit position. These maps are obtained by projecting all track intercepts into four pixels. High efficiency and fast charge carrier collection occur near the collection electrode but decrease asymmetrically towards the edges and corners. Particularly, the drop in charge collection speed, resulting in reduced efficiency, is located beneath the n-well of the analog front-end (see figure 1). While the n-wells in the digital readout circuitry are thin and uniformly distributed, the n-well in the analog front-end has a width of about 4 μm , which affects the electric field at the interface of the p-well and the low-dose n-implant layer, creating local potential wells that slow down charge collection. This does not influence charge sharing, and the cluster size map is therefore symmetric, as shown in figure 3c.

The simulations presented in figure 2a do not consider any well structure within the deep p-wells. In order to fully understand and reproduce the measurements presented here, more realistic

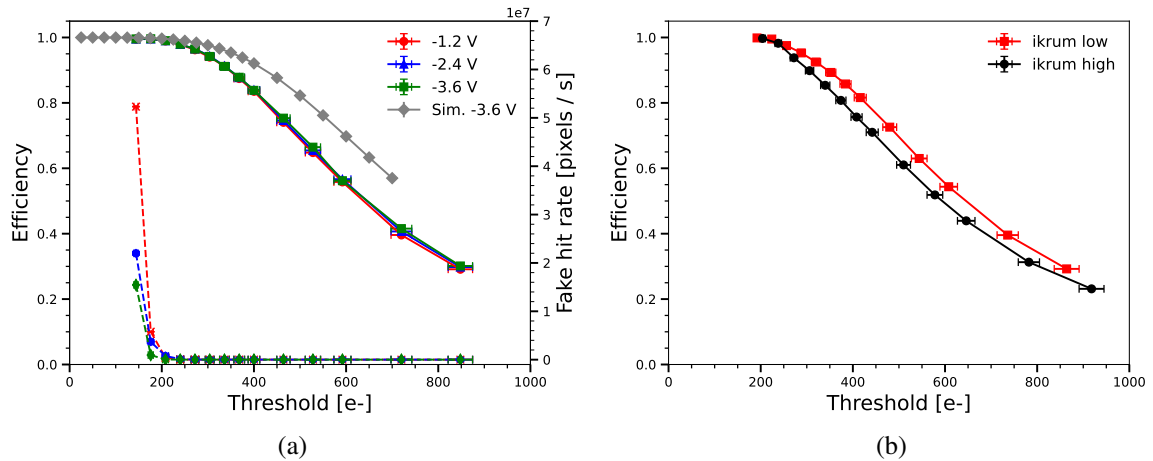


Figure 2: (a) Measured efficiency (left axis) in solid lines and fake hit rate (right axis) in dashed lines as a function of the hit detection threshold for three different sensor bias voltages in triggered mode. The expected efficiency at -3.6 V obtained from simulations with generic profiles is also shown. (b) Measured efficiency as a function of the hit detection threshold for two different Krummenacher currents in ToA mode. The sensor is biased at -1.2 V.

simulations, including the well of the analog front-end circuitry and its electronics simulations, have been performed. Those studies are summarized in [11].

Figure 4 illustrates the CSA output for slow and fast signals for large and small $ikrum$. The loss of the CSA output signal height for slow signals occurs due to a mismatch between the charge collection time and the CSA response time. This effect is known as ballistic deficit. While the signal amplitude for the fast signals barely depends on $ikrum$, slow signals yield a different amplitude. As a result, a low $ikrum$ improves the overall chip efficiency, as demonstrated in figure 2b. At low hit detection thresholds and larger bias voltages, the in-pixel response remains uniform, achieving an efficiency of 99.6% at a threshold of 144 electrons with the sensor biased at -3.6 V.

This effect is influenced by the fast analog front-end and the large pitch of H2M [11]. The integration time of a few nanoseconds contributes to the ballistic deficit by reducing the effective amplitude of slower signals compared to faster ones. Additionally, the large pitch of $35 \mu\text{m}$ results in significant spacing between the lateral electric field components of the collection electrodes and the gap, which makes it more sensitive to field perturbations due to the n-wells in the p-well region. This makes H2M the only chip in this technology where such non-uniform in-pixel responses have been observed.

4 Conclusion

The H2M test chip, manufactured using a modified 65 nm CIS, successfully ported a hybrid architecture with ToA and ToT counters in each pixel into a MAPS. Both the analog and the digital front-ends are fully functional. A single-pixel noise of 33 electrons r.m.s. and a threshold dispersion of 45 electrons for the equalized matrix has been measured, in agreement with predictions from

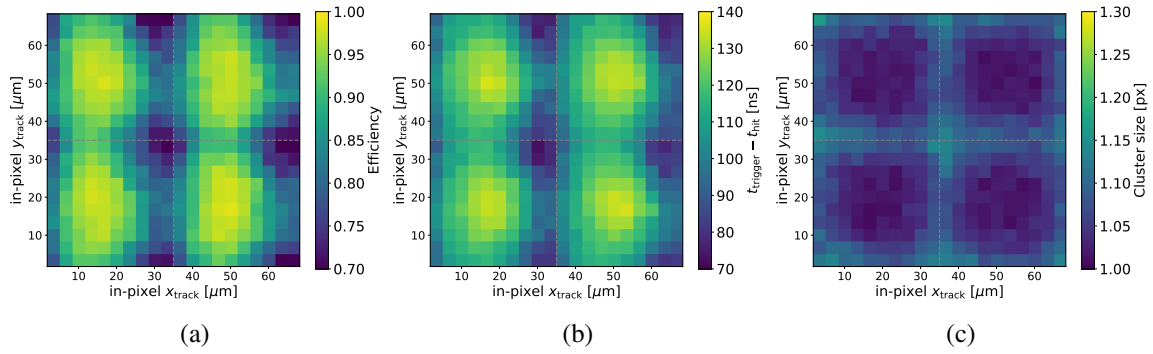


Figure 3: Measured efficiency (a), ToA (b), and cluster size (c) maps projected onto four pixels. In all figures, the sensor is biased at -1.2 V, and the hit detection threshold is 332 electrons. The pixel cell boundary is marked with a dashed gray line.

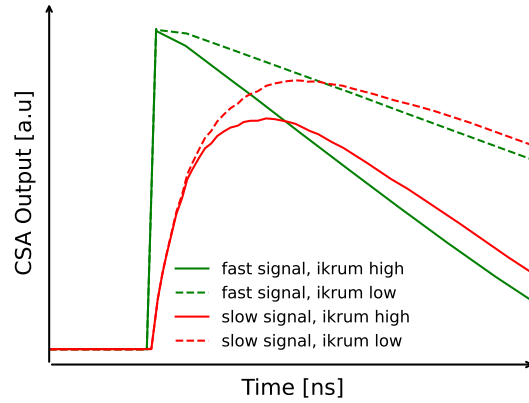


Figure 4: Sketch showing the different impact of the ballistic deficit on slow and fast signals.

front-end simulations. Test beam measurements showed a non-uniform in pixel response, with efficiency and timing strongly depending on the track impact position. This effect, amplified by the large pitch and fast front-end, has been correlated with the size and location of the n-wells of the analog circuitry. When operating the chip with high bias voltages and low $ikrum$, high efficiency, and uniform in-pixel response are achieved. Complementary measurements using laser and radioactive sources, along with simulations, have been conducted to better understand the influence of n-wells on charge collection and to prevent the issue from appearing in future chip submissions.

Acknowledgments

The measurements leading to these results have been performed at the Test Beam Facility at DESY Hamburg (Germany), a member of the Helmholtz Association (HGF).

The developments presented in this contribution are performed in collaboration with the CERN EP R&D programme on technologies for future experiments.

This project has received funding from the European Union’s Horizon 2020 Research and Innovation programme under GA no 101004761.

References

- [1] G. Aglieri Rinella et al., *Characterization of analogue Monolithic Active Pixel Sensor test structures implemented in a 65 nm CMOS imaging process*, Nucl. Instrum. Methods, **1069** (2024) 169896
- [2] G. Aglieri Rinella et al., *Digital pixel test structures implemented in a 65 nm CMOS process*, Nucl. Instrum. Methods, **1056** (2023) 168589
- [3] W. Snoeys et al., *Optimization of a 65 nm CMOS Imaging Process for Monolithic CMOS Sensors for High Energy Physics*, PoS, **Pixel2022** (2023) 83
- [4] F. Krummenacher, *Pixel detectors with local intelligence: an IC designer point of view*, Nucl. Instrum. Methods, **305** (1991) 527-532
- [5] T. Vanat et al., *Caribou — A versatile data acquisition system*, PoS, **TWEPP2020** (2020) 100
- [6] R. Diener et al., *The DESY II test beam facility*, Nucl. Instrum. Methods **922** (2019) 265
- [7] Y. Liu et al., *ADENIUM — A demonstrator for a next-generation beam telescope at DESY J*. Instr **18** (2023) P06025
- [8] H. Augustin et al., *TelePix – A fast region of interest trigger and timing layer for the EUDET Telescopes*, J. Instr. **1048** (2023), 167947
- [9] D. Dannheim et al., *Corryvreckan: a modular 4D track reconstruction and analysis software for test beam data*, J. Instr. **16** (2021), P03008
- [10] H. Wennl f et al., *Simulating Monolithic Active Pixel Sensors: A Technology-Independent Approach Using Generic Doping Profiles*, Accepted for publication in Nucl. Instrum. Methods
- [11] C. Lemoine et al., *Impact of the circuit layout on the charge collection in a monolithic pixel sensor*, submitted to J. Instr., **Pixel2024** (2025)